INFO #: 50707162

CustID: 3638
Fonterra Co-operative Group Limited
Interloans Librarian
Library
Private Bag 11029
Palmerston North , New Zealand .

Customer No:	**3638 / 87054**
Date of Order:	**03/03/2011**
Date of Shipping:	**03/03/2011**
Orderer:	**Interloans Librarian**
Department:	
Bill Ref:	**Sinclair, Sue**
Order No:	
Shipping method:	**eMail**
	interloans.pda@fonterra.com

Standard

Journal:	Nature
Citations:	569(7249 SUPPL: *):996-999 2009 june
Author:	Niethammor, et al
Title:	A tissue-scale gradient of hydrogen peroxide…….
ISSN:	00280836

LETTERS

A tissue-scale gradient of hydrogen peroxide mediates rapid wound detection in zebrafish

Philipp Niethammer[1]*, Clemens Grabher[2]*†, A. Thomas Look[2,3] & Timothy J. Mitchison[1]

Barrier structures (for example, epithelia around tissues and plasma membranes around cells) are required for internal homeostasis and protection from pathogens. Wound detection and healing represent a dormant morphogenetic program that can be rapidly executed to restore barrier integrity and tissue homeostasis. In animals, initial steps include recruitment of leukocytes to the site of injury across distances of hundreds of micrometres within minutes of wounding. The spatial signals that direct this immediate tissue response are unknown. Owing to their fast diffusion and versatile biological activities, reactive oxygen species, including hydrogen peroxide (H_2O_2), are interesting candidates for wound-to-leukocyte signalling. Here we probe the role of H_2O_2 during the early events of wound responses in zebrafish larvae expressing a genetically encoded H_2O_2 sensor[1]. This reporter revealed a sustained rise in H_2O_2 concentration at the wound margin, starting ~3 min after wounding and peaking at ~20 min, which extended ~100–200 μm into the tail-fin epithelium as a decreasing concentration gradient. Using pharmacological and genetic inhibition, we show that this gradient is created by dual oxidase (Duox), and that it is required for rapid recruitment of leukocytes to the wound. This is the first observation, to our knowledge, of a tissue-scale H_2O_2 pattern, and the first evidence that H_2O_2 signals to leukocytes in tissues, in addition to its known antiseptic role.

Hydrogen peroxide (H_2O_2) is a chemically relatively stable reactive oxygen species (ROS) that can diffuse in tissues and cross cell membranes[2], making it an interesting candidate for paracrine tissue signalling. Plants exploit H_2O_2 as a paracrine signal to regulate xylem differentiation and lignification[2]. The known signalling roles of H_2O_2 in animals are primarily within the cytoplasm, where it regulates metabolism, phosphatase activity and gene transcription, and causes oxidative damage at higher concentrations[3]. Paracrine signalling has been seen in cell culture experiments, but these may not faithfully mimic extracellular conditions in tissues[2].

To investigate possible paracrine signalling by H_2O_2, we imaged its spatiotemporal dynamics, together with leukocyte motility, in an intact vertebrate tissue subjected to mechanical wounding. The zebrafish larval tail fin has become a popular vertebrate model system to study inflammatory and regenerative responses to wounds[4–7]. Rapid leukocyte recruitment to the wound can be easily imaged, and the molecular dynamics of the tissue perturbed using morpholino knockdown, transgenic expression and pharmacology.

We measured H_2O_2 by expressing HyPer, a genetically encoded ratiometric sensor that is highly selective for H_2O_2 over other ROS[1]. HyPer consists of the bacterial H_2O_2-sensitive transcription factor OxyR fused to a circularly permuted yellow fluorescent protein (YFP). Cysteine oxidation of the OxyR part induces a conformational change that increases emission excited at 500 nm (YFP_{500}) and decreases emission excited at 420 nm (YFP_{420}). This change is rapidly reversible within the reducing cytoplasmic environment, allowing dynamic monitoring of intracellular H_2O_2 concentration. We introduced HyPer by messenger RNA injection into zebrafish embryos to induce global cytoplasmic expression (Fig. 1a) and confirmed that HyPer ratios respond to externally added H_2O_2 (Supplementary Fig. 1a).

Upon local injury of the tail fin of zebrafish larvae at 3 days post fertilization (3 d.p.f.), we observed a rapid and marked increase in HyPer ratio signal (YFP_{500}/YFP_{420}) at the wound margin (Fig. 1b and Supplementary Movie 1). To test if this was caused by a non-specific environmental effect (for example, pH change), we expressed YFP alone, and observed only a marginal fluorescence increase, most probably due to ruffling/contraction of the wound margin inducing a local increase in tissue thickness (Supplementary Fig. 1b). Similarly, the pH reporter BCECF-AM did not indicate a major contribution of pH to the wound margin signal. H_2O_2 production at the wound margin was confirmed by using the H_2O_2-selective fluorogenic probe acetyl-pentafluorobenzene sulphonyl fluorescein[8] (Supplementary Fig. 1c). Hence, the primary wound margin signal is due to H_2O_2 or a closely related molecule—HyPer does not respond to superoxide (O_2^-) or nitric oxide (NO)[1]. The H_2O_2 signal peaked ~20 min after wounding (Fig. 1c). At this time, the observable H_2O_2 gradient extended ~100–200 μm inward from the wound margin (Fig. 1d), so that its low concentration end approached the nearest blood vessel.

We quantified leukocyte recruitment to the wound by imaging transmitted light and two different leukocyte-specific fluorescent tags: *mpo::GFP* (ref. 9) (Figs 2d and 3c) and *lysC::DsRED2* (ref. 10) (Fig. 1e). Some leukocytes were located in the fin at the time of wounding, whereas others were apparently recruited from the vasculature. Excluding occasional cases where a leukocyte was already present at the wound site, the first leukocyte arrived at the wound margin 17 ± 6 min after wounding (mean ± s.d. of $n = 14$ larvae). This timing is superimposed on a typical H_2O_2 profile in Fig. 1c. Wound margin H_2O_2 production clearly preceded recruitment of the first leukocyte in most cases (see also Fig. 1e, Supplementary Fig. 1d and Supplementary Movie 2), indicating that the source of H_2O_2 must be tail-fin epithelial cells, not leukocytes. This finding runs counter to the prevailing view that ROS production during inflammatory responses originates from leukocyte oxidative bursts[11].

The main physiological source of extracellular H_2O_2 is likely to be NADPH oxidases, which transport electrons from cytoplasmic NADPH to generate O_2^- or H_2O_2 in phagosomes or outside the cell[12]. The zebrafish genome encodes Nox1, Nox2 (leukocyte oxidase), Nox4, Nox5 and a single isoform of Duox[13] (Fig. 2a). Nox1–5 generate superoxide, which can be dismutated into H_2O_2 by separate superoxide

[1]Department of Systems Biology, Harvard Medical School, Boston, [2]Department of Pediatric Oncology, Dana-Farber Cancer Institute, Harvard Medical School, Boston, Massachusetts 02115, USA. [3]Division of Hematology/Oncology, Department of Pediatrics, Children's Hospital, Harvard Medical School, Boston, Massachusetts 02114, USA. †Present address: Karlsruhe Institute of Technology, Forschungszentrum Karlsruhe GmbH, Institute of Toxicology and Genetics, 76344 Eggenstein-Leopoldshafen, Germany.
*These authors contributed equally to this work.

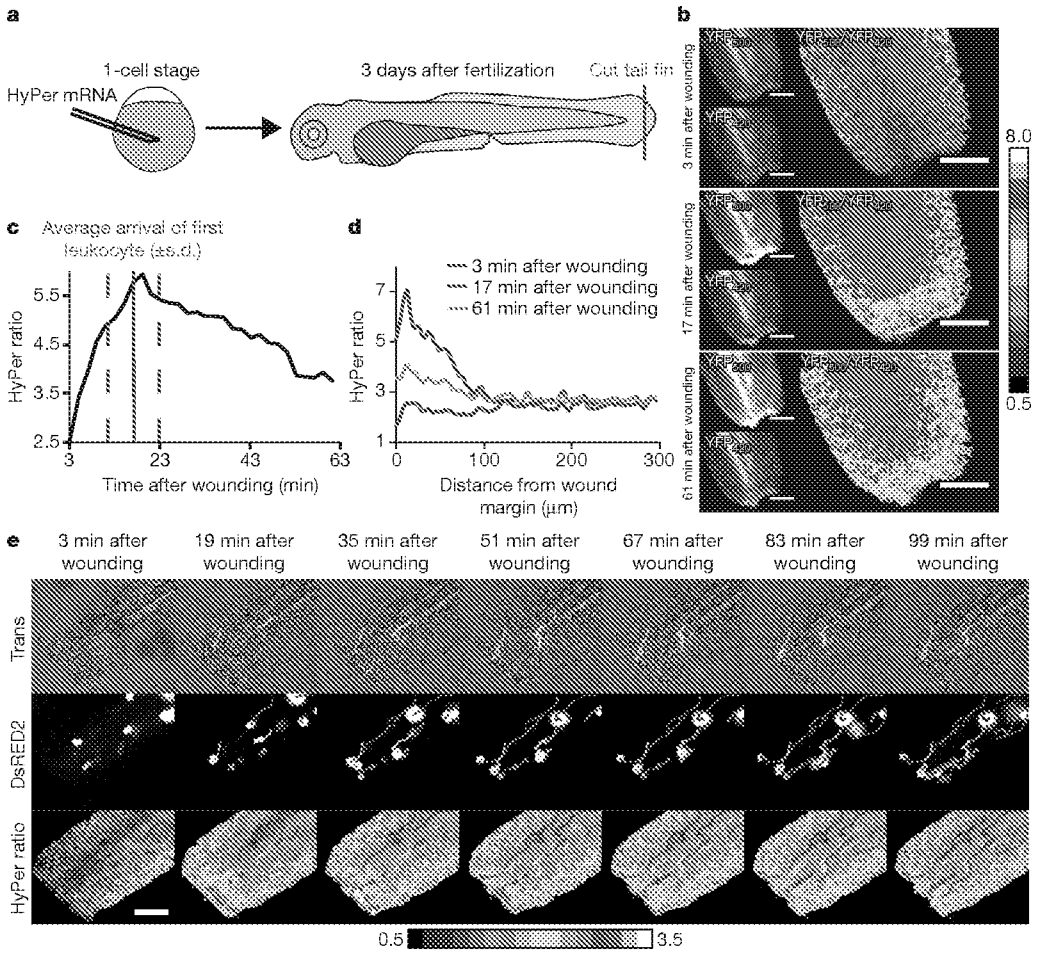

Figure 1 | Wound margin H_2O_2 production in zebrafish larvae. **a**, Experimental procedure. **b**, HyPer imaging in an injured zebrafish larva. $[H_2O_2]$ is inferred from the YFP_{500}/YFP_{420} excitation ratio of HyPer. Greyscale scaling is adjusted to improve contrast. **c**, Temporal $[H_2O_2]$ profile in a ~10–30-μm broad region of interest along the wound margin. Arrival of first leukocyte at wound (solid red line) ± s.d. (dashed red line) is shown. **d**, $[H_2O_2]$ line profile normal to the wound margin. **e**, Imaging of leukocyte recruitment and $[H_2O_2]$ in a *lysC::DsRED2* fish line[10]. Coloured lines are superimposed leukocyte tracks. Pseudo-colour calibration bars: HyPer ratio (YFP_{500}/YFP_{420}). Scale bars: 100 μm.

dismutase (SOD) enzymes, whereas Duox generates H_2O_2 without requiring a separate SOD[14]. To test for a role of any Nox enzyme in generating wound margin H_2O_2, we added two structurally unrelated small molecule inhibitors of the whole family, diphenyleneiodonium (DPI) and VAS2870[15–18], to the bathing water before wounding. Both efficiently inhibited H_2O_2 production without obvious toxicity (Fig. 2b, c; see also Supplementary Movie 3).

We next quantified leukocyte recruitment in the *mpo::GFP* fish line[9] during the peak period of H_2O_2 production. Under control conditions, an average of 4–6 leukocytes arrived at the wound margins within the first 42 min after wounding. Nox inhibition strongly attenuated leukocyte recruitment to the wound during this initial phase of the response, with less than one leukocyte arriving, on average, in drug-treated larvae (Fig. 2d, e and Supplementary Movie 4).

The specific Nox that generates wound margin H_2O_2 was identified by targeting pre-mRNA splice sites with antisense morpholinos. Interference with pre-mRNA splicing of $P22^{phox}$ (*cyba*), an essential subunit of Nox1–4 (ref. 12), led to quantitative conversion of its mRNA level into a mutant with a premature stop codon that probably terminated translation of $P22^{phox}$ after the 28th amino acid residue (Supplementary Fig. 2c, inset). This had no effect on the H_2O_2 gradient (Supplementary Fig. 2a–c and Supplementary Movie 5) or leukocyte recruitment to the wound (Supplementary Fig. 2d). Nox5 and Duox remained as candidates. By semi-quantitative polymerase chain reaction (PCR) we confirmed that *duox* but not *nox5* is expressed in tail-fin tip tissue (Supplementary Fig. 3c). In mammals, DUOX is mainly expressed in the thyroid gland, where it generates H_2O_2 for organification of I^- (ref. 19), but also in epithelial surfaces that contact liquid environments, including the luminal surface of the gut and lung. Extracellular H_2O_2 made by DUOX is thought to react with halide or thiocyanate, catalysed by secreted lactoperoxidases, to generate more ROS that kill luminal bacteria[20,21]. DUOX contains two Ca^{2+} binding EF-hand motifs and, at least in cell culture, can be activated by Ca^{2+}-mobilizing small molecules[22] and by mechanical cell injury[23], making it a good candidate for wound signalling.

Morpholino-induced perturbation of *duox* pre-mRNA splicing (Fig. 3b, inset) caused a developmental morphology phenotype characterized by cell death predominantly in the head region. This phenotype is probably specific for *duox* knockdown, because two independent splice morpholinos, but not a corresponding 5-misprime morpholino, induced the same phenotype (not shown). To generate morphologically normal tail fins for the assay, we simultaneously knocked down *p53*, which partially rescued the *duox* knockdown morphological phenotype. Notably, we found a significant reduction of wound-induced H_2O_2 production in *duox/p53* knockdown larvae compared with *duox 5-MP/p53* controls (Fig. 3a, b, Supplementary Fig. 2a and Supplementary Movie 6). Furthermore, *duox* knockdown strongly attenuated recruitment of leukocytes to the wound (Fig. 3c, d and Supplementary Movies 7 and 8). This attenuation was not caused by a reduction of total leukocyte number in *duox* knockdown larvae (Supplementary Fig. 2e). *Duox* knockdown did cause a significant reduction in the number of

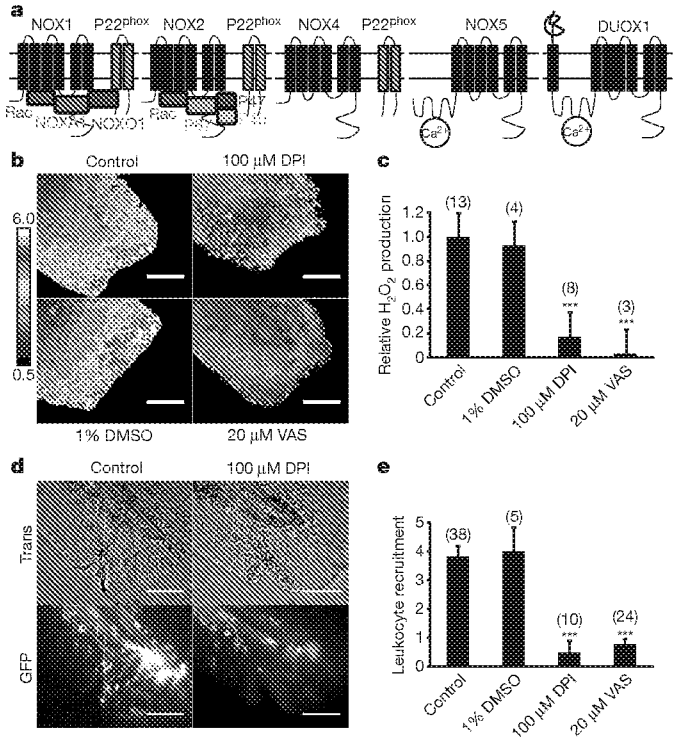

Figure 2 | Nox/Duox activity is required for wound margin H_2O_2 production and leukocyte recruitment. **a**, Scheme of mammalian NADPH oxidases also found in zebrafish[12,13]. **b**, Wound margin $[H_2O_2]$ with/without DPI or VAS2870 (VAS), or carrier (1% DMSO), imaged 17 min after wounding. Pseudo-colour calibration bar: HyPer ratio (YFP_{500}/YFP_{420}). **c**, Statistical quantification of wound margin $[H_2O_2]$. **d**, Injured tail fins of *mpo::GFP* larvae[9] with/without DPI (42 min after wounding). Coloured lines are leukocyte tracks derived from the corresponding time-lapse movies. **e**, Statistical quantification of leukocyte recruitment to wound margin. Error bars indicate s.e.m. of indicated number of larvae (brackets). Triple asterisk, $P < 0.001$ (versus control). Scale bars: 100 μm.

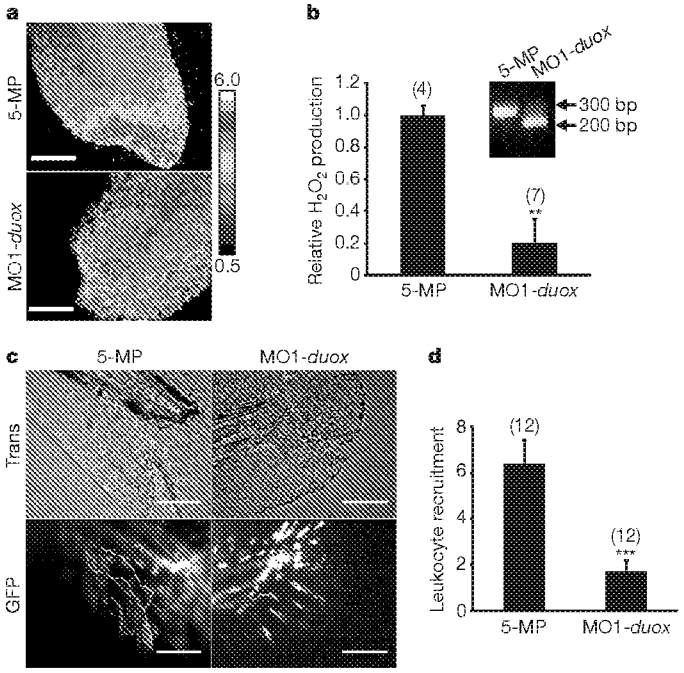

Figure 3 | Duox activity is required for wound margin H_2O_2 production and leukocyte recruitment. **a**, Wound margin H_2O_2 after morpholino-mediated *duox* knockdown (MO1-*duox*) or injection of a corresponding 5-misprime morpholino (5-MP) imaged 17 min after wounding. Inset: RT–PCR of a *duox* mRNA region flanking the targeted splice site. Pseudo-colour calibration bar: HyPer ratio (YFP_{500}/YFP_{420}). **b**, Quantification of wound margin $[H_2O_2]$. **c**, Injured tail fins of *mpo::GFP* larvae[9] injected with MO1-*duox*, or 5-MP (42 min after wounding). Coloured lines are leukocyte tracks. **d**, Quantification of leukocyte recruitment. Error bars indicate s.e.m. of indicated number of larvae (brackets). Double asterisk, $P < 0.01$; triple asterisk, $P < 0.001$ (versus control). Scale bars: 100 μm.

leukocytes infiltrating the tail fin after wounding, reducing it to near the level seen in unwounded fins (Supplementary Fig. 3a). It also caused a significant decrease in directional migration towards the wound, whereas basal leukocyte motility, as observed in the absence of a wound, was not affected. These data implicate Duox as the main source of wound margin H_2O_2 required for rapid leukocyte recruitment.

We have visualized, for the first time, a tissue-scale gradient of H_2O_2 induced by wounding, found that it is generated by Duox activity in epithelial cells, and shown that it is required for leukocyte recruitment to the wound. On the basis of published calibration of HyPer in tissue culture[1], wound-induced extracellular H_2O_2 may reach concentrations of ~0.5–50 μM near the wound margin. The gradient was established within 10 min of wounding, and gradually dissipated over ~1–2 h. Visual inspection of movies (Figs 1e, 2d and 3c) suggested that leukocytes sensed the wound within ~10 min, from distances as large as 200 μm. Thus, the spatiotemporal scales of the H_2O_2 gradient and the leukocyte response were roughly similar. Trajectory analysis showed that the H_2O_2 gradient stimulated leukocyte recruitment mainly by increasing directionality of leukocyte migration and tissue infiltration (Supplementary Fig. 3a and Supplementary Movies 4 and 8). This argues against a permissive role of extracellular H_2O_2 for basal leukocyte motility in our assay, and favours the idea that wound margin H_2O_2 production spatially instructs rapid wound recruitment of leukocytes, either by direct chemotactic signalling or by stimulating production of a downstream chemoattractant. Direct chemotactic activity of H_2O_2 was previously demonstrated *in vitro* for neutrophils[24] and vascular smooth muscle cells[25] at concentrations[24] (~10 μM) that are roughly consistent with our estimation of wound margin $[H_2O_2]$. Together with our data, this raises the possibility that H_2O_2 itself acts as a paracrine, chemotactic signal during the initial phase of wound detection. Leukocytes might express trans-membrane receptors for H_2O_2—none are known, but T-type Ca^{2+} channels are thought to have this function in sensory neurons[26]. Alternatively, H_2O_2 might direct migration by entering the cytoplasm and locally modifying intracellular receptors, such as the redox-sensitive phosphatase PTEN[27]. Phosphatidylinositol-3,4,5-trisphosphate phosphatases such as PTEN or SHIP1 are thought to be important regulators of chemo- and electrotactic responses[28–30]. Our current data do not distinguish whether the spatial H_2O_2 gradient reflects diffusion from a localized source at the wound margin combined with global breakdown by catalases and/or peroxidases, or rather a gradient of H_2O_2 production induced by some upstream regulatory pattern, such as an electric field or a spatial gradient of an upstream signalling molecule. DUOX was previously implicated in constitutive ROS-induced microbial killing by mucosal epithelia[19]. Our data implicate it, for the first time, as a major, non-myeloid ROS source in the initial phase of inflammation. We hypothesize that the DUOX/lactoperoxidase system evolved to have two useful roles in early responses to epithelial wounding: local killing of invading bacteria, and rapid recruitment of phagocytic leukocytes from distant sites.

METHODS SUMMARY

Imaging of H_2O_2 and leukocytes in zebrafish. One-cell-stage zebrafish embryos were injected with HyPer mRNA. 3 d.p.f. larvae were subjected to tail-fin tip amputation and mounted in 1% low-melting agarose. HyPer fluorescence was excited with 501/16 and 420/40 band-pass excitation filters and corresponding YFP emission was acquired every 2 min within 3–42 min after injury using a 535/30 band-pass emission filter. For calculating HyPer ratio images, YFP_{500} and

YFP_{420} images were smoothed, background subtracted, thresholded, and then divided.

Leukocytes were imaged every 30 s within 3–42 min after tail-fin incision of fluorescent leukocyte reporter zebrafish larvae. Leukocyte migration to the wound was observed both by fluorescence and transmission imaging. Final leukocyte count at the wound margin was assessed 42 min after injury.

Zebrafish larvae were anaesthetized for wounding and imaging experiments. All media were sterile filtered. Blades were treated with 70% ethanol before use. Imaging was optimized for low illumination, and performed on an inverted wide-field microscope equipped with a CCD camera and a mercury illumination source.

Genetic and pharmacological perturbations. Anaesthetized larvae were incubated with pharmacological compounds up to 40 min before wounding and during imaging. Antisense morpholinos were injected into 1-cell-stage embryos. Morpholino-mediated splice perturbation was confirmed by RT–PCR.

Full Methods and any associated references are available in the online version of the paper at www.nature.com/nature.

Received 17 March; accepted 23 April 2009.
Published online 3 June 2009.

1. Belousov, V. V. *et al.* Genetically encoded fluorescent indicator for intracellular hydrogen peroxide. *Nature Methods* **3,** 281–286 (2006).
2. Bienert, G. P., Schjoerring, J. K. & Jahn, T. P. Membrane transport of hydrogen peroxide. *Biochim. Biophys. Acta* **1758,** 994–1003 (2006).
3. Oktyabrsky, O. N. & Smirnova, G. V. Redox regulation of cellular functions. *Biochemistry* **72,** 132–145 (2007).
4. Redd, M. J., Cooper, L., Wood, W., Stramer, B. & Martin, P. Wound healing and inflammation: embryos reveal the way to perfect repair. *Phil. Trans. R. Soc. Lond. B* **359,** 777–784 (2004).
5. Renshaw, S. A., Loynes, C. A., Elworthy, S., Ingham, P. W. & Whyte, M. K. Modeling inflammation in the zebrafish: how a fish can help us understand lung disease. *Exp. Lung Res.* **33,** 549–554 (2007).
6. Grabher, C. *et al.* Birth and life of tissue macrophages and their migration in embryogenesis and inflammation in medaka. *J. Leukoc. Biol.* **81,** 263–271 (2007).
7. Huttenlocher, A. & Poznansky, M. C. Reverse leukocyte migration can be attractive or repulsive. *Trends Cell Biol.* **18,** 298–306 (2008).
8. Maeda, H. *et al.* Fluorescent probes for hydrogen peroxide based on a non-oxidative mechanism. *Angew. Chem. Int. Edn Engl.* **43,** 2389–2391 (2004).
9. Mathias, J. R. *et al.* Resolution of inflammation by retrograde chemotaxis of neutrophils in transgenic zebrafish. *J. Leukoc. Biol.* **80,** 1281–1288 (2006).
10. Hall, C., Flores, M. V., Storm, T., Crosier, K. & Crosier, P. The zebrafish lysozyme C promoter drives myeloid-specific expression in transgenic fish. *BMC Dev. Biol.* **7,** 42 (2007).
11. Sen, C. K. & Roy, S. Redox signals in wound healing. *Biochim. Biophys. Acta* **1780,** 1348–1361 (2008).
12. Bedard, K. & Krause, K. H. The NOX family of ROS-generating NADPH oxidases: physiology and pathophysiology. *Physiol. Rev.* **87,** 245–313 (2007).
13. Kawahara, T., Quinn, M. T. & Lambeth, J. D. Molecular evolution of the reactive oxygen-generating NADPH oxidase (Nox/Duox) family of enzymes. *BMC Evol. Biol.* **7,** 109 (2007).
14. Ameziane-El-Hassani, R. *et al.* Dual oxidase-2 has an intrinsic Ca^{2+}-dependent H_2O_2-generating activity. *J. Biol. Chem.* **280,** 30046–30054 (2005).
15. ten Freyhaus, H. *et al.* Novel Nox inhibitor VAS2870 attenuates PDGF-dependent smooth muscle cell chemotaxis, but not proliferation. *Cardiovasc. Res.* **71,** 331–341 (2006).
16. Stielow, C. *et al.* Novel Nox inhibitor of oxLDL-induced reactive oxygen species formation in human endothelial cells. *Biochem. Biophys. Res. Commun.* **344,** 200–205 (2006).
17. Lange, S. *et al.* Platelet-derived growth factor BB stimulates vasculogenesis of embryonic stem-cell-derived endothelial cells by calcium-mediated generation of reactive oxygen species. *Cardiovasc. Res.* **81,** 159–168 (2009).
18. Tegtmeier, F. *et al.* Compounds containing a N-heteroaryl moiety linked to fused ring moieties for the inhibition of NAD(P)H oxidases and platelet activation. Patent WO/2005/111041 (2005).
19. Donko, A., Peterfi, Z., Sum, A., Leto, T. & Geiszt, M. Dual oxidases. *Phil. Trans. R. Soc. Lond. B* **360,** 2301–2308 (2005).
20. Geiszt, M., Witta, J., Baffi, J., Lekstrom, K. & Leto, T. L. Dual oxidases represent novel hydrogen peroxide sources supporting mucosal surface host defense. *FASEB J.* **17,** 1502–1504 (2003).
21. Ha, E. M., Oh, C. T., Bae, Y. S. & Lee, W. J. A direct role for dual oxidase in *Drosophila* gut immunity. *Science* **310,** 847–850 (2005).
22. Forteza, R., Salathe, M., Miot, F., Forteza, R. & Conner, G. E. Regulated hydrogen peroxide production by Duox in human airway epithelial cells. *Am. J. Respir. Cell Mol. Biol.* **32,** 462–469 (2005).
23. Wesley, U. V., Bove, P. F., Hristova, M., McCarthy, S. & van der Vliet, A. Airway epithelial cell migration and wound repair by ATP-mediated activation of dual oxidase 1. *J. Biol. Chem.* **282,** 3213–3220 (2007).
24. Klyubin, I. V., Kirpichnikova, K. M. & Gamaley, I. A. Hydrogen peroxide-induced chemotaxis of mouse peritoneal neutrophils. *Eur. J. Cell Biol.* **70,** 347–351 (1996).
25. Li, W., Liu, G., Chou, I. N. & Kagan, H. M. Hydrogen peroxide-mediated, lysyl oxidase-dependent chemotaxis of vascular smooth muscle cells. *J. Cell. Biochem.* **78,** 550–557 (2000).
26. Todorovic, S. M. *et al.* Redox modulation of T-type calcium channels in rat peripheral nociceptors. *Neuron* **31,** 75–85 (2001).
27. Kwon, J. *et al.* Reversible oxidation and inactivation of the tumor suppressor PTEN in cells stimulated with peptide growth factors. *Proc. Natl Acad. Sci. USA* **101,** 16419–16424 (2004).
28. Zhao, M. *et al.* Electrical signals control wound healing through phosphatidylinositol-3-OH kinase-γ and PTEN. *Nature* **442,** 457–460 (2006).
29. Subramanian, K. K. *et al.* Tumor suppressor PTEN is a physiologic suppressor of chemoattractant-mediated neutrophil functions. *Blood* **109,** 4028–4037 (2007).
30. Nishio, M. *et al.* Control of cell polarity and motility by the PtdIns(3,4,5)P_3 phosphatase SHIP1. *Nature Cell Biol.* **9,** 36–44 (2007).

Supplementary Information is linked to the online version of the paper at www.nature.com/nature.

Acknowledgements P.N. was supported by a Human Frontiers Science Program long-term fellowship. This work was supported by the National Institutes of Health grant GM023928. We would like to thank A. Huttenlocher and P. Crosier for providing us with the *mpo::GFP* and *lysC::DsRED2* transgenic zebrafish lines, respectively.

Author Contributions P.N. and T.J.M. conceived the project. P.N. and C.G. designed and executed the experiments. C.G. and A.T.L. contributed expertise in the zebrafish system. P.N. and T.J.M. contributed expertise in imaging and pharmacology. T.J.M. and A.T.L. provided guidance and institutional support. P.N., C.G. and T.J.M. wrote the text.

Author Information Reprints and permissions information is available at www.nature.com/reprints. Correspondence and requests for materials should be addressed to P.N. (Philipp_Niethammer@hms.harvard.edu).

METHODS

General fish procedures. Zebrafish strains AB, *mpo::GFP* (ref. 9) and *lysC::DsRED2* (ref. 10) were maintained as described[31]. For wounding assays, zebrafish were anaesthetized in E3 (5 mM NaCl, 0.17 mM KCl, 0.33 mM $CaCl_2$, 0.33 mM $MgSO_4$) containing 0.1 mg ml^{-1} Tricaine (Sigma) before wounding. To prevent pigment formation, larvae were maintained in E3 containing 0.2 mM *N*-phenylthiourea (PTU; Sigma). All buffers were sterile filtered and blades were sterilized using 70% ethanol before use.

Imaging the wound response. For all imaging, larvae were maintained in E3 supplemented with 0.1 mg ml^{-1} Tricaine.

For imaging of H_2O_2 production, 1-cell-stage zebrafish embryos were injected with HyPer^{l} mRNA (~0.5 mg ml^{-1}). 3 d.p.f. larvae were subjected to tail-fin tip amputation using a needle knife (Fine Science Tools) and embedded in 1% low melting agarose (Lonza) in a glass-bottom dish (Matek Corporation). Every 2 min starting ~3 min after wounding, HyPer fluorescence was excited using 420/40 and 501/16 band-pass filters (Chroma), and YFP emission was acquired using a 535/30 band-pass filter.

For alternative H_2O_2 imaging, 2–3 d.p.f. larvae were loaded ~60 min with 50 μM acetyl-pentafluorobenzene sulphonyl fluorescein (Calbiochem) before wounding. Emission was excited using a 484/15 band-pass filter (Chroma) and acquired using a 525/50 band-pass filter (Chroma).

For pH imaging, 2–3 d.p.f. larvae were loaded ~60 min with 50 μM 3′-*O*-acetyl-2′,7′-bis(carboxyethyl)-4 or 5-carboxyfluorescein diacetoxymethyl ester (BCECF-AM, Calbiochem) before wounding. Emission was excited using a 484/15 band-pass filter (Chroma) and acquired using a 535/30 band-pass filter (Chroma). For imaging of leukocyte recruitment, 3–5 d.p.f. *mpo::GFP* or *lysC::DsRED2* larvae were cut at the tail fin using a tungsten needle (Fine Science Tools), mounted in agarose, and leukocyte fluorescence was excited using a 484/15 or 540/15 band-pass filter (Chroma). Emission was acquired every 30 s using a 525/50 or 610/80 band-pass filter (Chroma). All images were acquired at room temperature (~26 °C) using Metamorph (Molecular Devices) and a Nikon Eclipse TE300 microscope equipped with 20× plan-apochromate NA 0.75 air objective lens, an ORCA-ER camera (Hamamatsu), and a mercury light source (Chiu Technical Corporation).

Tail-fin tip amputation (needle blade) was used in all HyPer assays; tail-fin incision (tungsten needle) in all chemotaxis assays. Only the same types of cuts were directly compared. The HyPer signal was not dependent on the type of cut (Supplementary Fig. 3b).

Generally, each imaging set-up was optimized for minimal light exposure of larvae. Whenever possible, we used two neutral density filters (except for BCECF-AM where dye loading was rather inefficient, so that we had to use one neutral density filter), highest camera gain, and high binning (for example, 8× bin for probe imaging, 4× bin for leukocyte imaging).

Image processing and data analysis. For calculating HyPer ratio images, smoothed (one-pass median filter), background subtracted and thresholded YFP_{500} and YFP_{420} images were divided (YFP_{500}/YFP_{420}) using ImageJ (NIH) or Matlab (Mathworks). Upregulation of H_2O_2 was calculated by dividing the mean ratio acquired in a region of interest directly at the wound margin (r_{wound}) by the mean basal ratio acquired in a region of interest inside the body (r_{basal}, ~300–400 μm distant from the wound margin). H_2O_2 upregulation was expressed either as multiple ($f_{mult} = r_{wound}/r_{basal}$; for example, Supplementary Fig. 2b) or fraction of the base level ($f_{fract} = (r_{wound} - r_{basal})/r_{basal}$). Relative H_2O_2 production at wound margin (for example, Figs 2c and 3b) was derived as f_{fract} normalized to the control ($f_{rel} = f_{fract}(sample)/f_{fract}(control)$).

Leukocyte recruitment was determined by counting all migrating cells that arrived at the wound margin within 42 min after wounding as judged from the 30 s per frame time-lapse movies of *mpo::GFP* leukocyte reporter fish (transmission and GFP channel). Cells that already resided at the wound margin at the beginning of the time-lapse sequence (~3 min after wounding) were not counted.

Leukocyte trajectory analysis. Trajectory analysis was performed on the same leukocyte time-lapse data that were also used to quantify wound recruitment of leukocytes. Trajectories were generated by marking the approximate centre of mass of those cells that moved in the ventral tail fin, and could be identified with adequate reliability. Only those cells were included in the statistical path analysis that described a path of at least 50 μm. Furthermore, tracks or part of tracks within a radius of 50 μm around the centre of mass of the triangular wound region were not included into the analysis to avoid tracking of cells that had already reached the wound, and merely moved along the wound margins. Average velocity (v_{av}) was calculated as $v_{av} = l_{track}/t_{track}$, with l_{track} being the length of the track and t_{track} being the total track time.

Path linearity (which is frequently also termed 'directionality') was calculated as $Dir_p = d_{OE}/l_{track}$, with d_{OE} being the Euclidian distance between origin (O) and endpoint (E) of the track.

Wound directionality was calculated as $Dir_w = (d_{OW} - d_{EW})/l_{track}$, with d_{OW} being the distance between track origin and centre of mass of the wound (W), and d_{EW} being the distance between track endpoint and W.

Pharmacological and morpholino treatments. Larvae were incubated in E3 supplemented with 100 μM DPI (Sigma), 20 μM VAS2870, 1% DMSO (Sigma) 30–40 min before wounding. Mounting agarose and imaging medium (E3) were supplemented with the indicated compound concentrations.

The following splice morpholinos (Gene Tools) were injected into 1-cell-stage larvae (~0.5–1 mM): MO-*cyba*, 5′-ATCATAGCATGTAAGGATACATCCC-3′; MO1-*duox*, 5′-AGTGAATTAGAGAAATGCACCTTTT-3′; MO5-MP-*duox* (5-MP), 5′-AGTcAATTAcAGAAATcCAgCTaTT-3′; MO2-*duox*, 5′-ACATTC ACTCTCTCACCTGGATATG-3′. Lower-case letters indicate base-pair mismatch with the target sequence.

For morphotyping, RNA was prepared from 3 d.p.f. larvae by phenol-chloroform extraction (TRI solution, Ambion), and one-step RT–PCR (Qiagen) was performed to confirm knockdown efficiency using the following primers: *cyba* forward, 5′-GCGAAGATTGAGTGGGCGATGTGGGCC-3′; *cyba* reverse, 5′-TTATTCGTTGATGGTGACAGACATAGGATTGTC-3′; *duox* forward, 5′-ACACATGTGACTTCATATCCAG-3′; *duox* reverse, 5′-ATTATTAAC TCATCCACATCCAG-3′.

The RT–PCR products were sequenced. MO-*cyba*-mediated splice perturbation produced a 146-bp deletion in the *cyba* mRNA, introducing a premature stop codon into the resulting splice-mutant mRNA, coding for a 28-amino-acid truncated translation product. MO1-*duox*-mediated splice perturbation produced a 39-bp in-frame deletion within the peroxidase-like domain of *duox*. MO1-*duox* and MO2-*duox* produced identical phenotypes; however, MO2-*duox*-injected larvae yielded neither detectable wild-type nor splice-mutant amplification product, whereas *beta-actin* could successfully be amplified from the same template. This indicated that MO2-*duox* resulted in *duox* mRNA knockdown, either by generating a splice-mutant mRNA that was rapidly degraded or that was too large to be amplified under our conditions. For phenotypical rescue of the tail fin in the HyPer and leukocyte migration assays, MO1-*duox* and MO5-MP-*duox* (5-MP) morpholinos were generally co-injected with a morpholino inhibiting *p53* mRNA translation (~0.2 mM, 5′-GCG CCATTGCTTTGCAAGAATTG-3′[32]).

Cell sorting. Larvae (~150) were collected from Tg(*mpo::GFP*) at 80 h.p.f. and disaggregated into a single-cell suspension as previously described[33]. Sorting of *mpo::GFP* positive cells was performed on a BD Aria based on GFP fluorescence.

RNA isolation and semi-quantitative RT–PCR. Total RNA from amputated tail fins (80 h.p.f.) or sorted GFP^+ cells was extracted with TRIzol (Invitrogen). RT–PCR was performed with a one-Step RT–PCR kit (Qiagen) according to the manufacturer's protocol using 35 cycles on 2 ng total RNA with intron-spanning primers. Oligo sequences were as follows: *duox* forward, 5′-GTTGGCTT TGGTGTAACTGTA-3′; *duox* reverse, 5′-GCCCAGGCTGTGAGAG-3′; *nox5* forward, 5′-TGGCCTAATGGTGGTCTGTTC-3′; *nox5* reverse, 5′-CAGAGC CGAAACCCAGATG-3′; *beta-actin* forward, 5′-CATTGGCAATGAGCGTT TC-3′; *beta-actin* reverse, 5′-TACTCCTGCTTGCTGATCCAC-3′.

Statistics. All error bars indicate standard errors of means (s.e.m.). All *P*-values have been derived by an unpaired, two-tailed *t*-test assuming unequal variances (heteroscedastic) using Excel (Microsoft).

31. Nusslein-Volhard, C. & Dahm, R. Zebrafish (Oxford Univ. Press, 2002).
32. Chen, J. *et al.* Loss of function of def selectively up-regulates Delta113p53 expression to arrest expansion growth of digestive organs in zebrafish. *Genes Dev.* 19, 2900–2911 (2005).
33. Bertrand, J. Y. *et al.* Definitive hematopoiesis initiates through a committed erythromyeloid progenitor in the zebrafish embryo. *Development* 134, 4147–4156 (2007).